Rapid design of miniaturised branch-line couplers through concurrent cell optimisation and surrogate-assisted fine-tuning

Slawomir Koziel[1] ✉, Piotr Kurgan[2]

[1]Engineering Optimization & Modeling Center, Reykjavik University, 101 Reykjavik, Iceland
[2]Faculty of Electronics, Telecommunications and Informatics, Gdansk University of Technology, 11/12 Narutowicza Street, 80-233 Gdansk, Poland
✉ E-mail: koziel@ru.is

Abstract: In this study, the authors introduce a methodology for low-cost simulation-driven design optimisation of highly miniaturised branch-line couplers (BLCs). The first stage of their design approach exploits fast concurrent optimisation of geometrically dependent, but electromagnetically isolated cells that constitute a BLC. The cross-coupling effects between the cells are taken into account in the second stage, where a surrogate-assisted fine-tuning procedure is executed. The tuning process is based on space-mapping-enhanced low-fidelity model of the entire BLC. The latter is constructed by cascading local response surface approximations (RSAs) of the BLC building blocks. The efficiency of their technique is demonstrated through the design of two compact BLCs. A considerable scale of miniaturisation has been achieved in both cases (83.7 and 87.4%, respectively), at the computational cost corresponding to a few EM simulations of the respective BLC. Comparison of numerical results with several surrogate-based design approaches as well as an experimental verification of the final designs are also provided.

1 Introduction

The development of reliable design methodologies for miniaturised microwave passives has been motivated by industrial demands for small-size and high-performance components to be used in a variety of modern wireless communication systems [1–3]. The main objective is to find a design that satisfies a given specification, using limited computational resources, and providing highly accurate results. However, the realisation of this goal has proven to be extremely challenging from the methodological standpoint.

A typical microwave circuit with reduced physical dimensions is constructed from composite structures that mimic – in term of complex scattering parameters – uniform transmission lines (TLs) in a limited frequency range [2–28]. Most commonly, T- [2, 4–11] or π-shaped [2, 8, 12–17] topologies are chosen for the composite structure realisation. Also, their various modifications, for example, including stepped-impedance sections, can be found in the literature [5, 6, 18–23]. These rather simple networks can be easily analysed by means of TL theory, which offers a relatively good approximation to the solution of the corresponding electromagnetic (EM) problem, assuming the lack of cross-coupling effects and a negligible influence of TL discontinuities on the performance of the entire microwave component. This, however, is acceptable only for conventional circuits [24]. When dealing with highly-miniaturised passives, characterised by complex and densely arranged layouts, the exploitation of simplified theoretical models is useful only to provide initial design solutions that require further EM fine-tuning [4–9, 11, 15, 16, 20, 21, 23]. In order to yield reliable results, it is preferable to apply a high-fidelity EM analysis from the early stages of the design process of compact microwave components [25, 26]. In other words, EM-driven optimisation of the entire miniaturised structure is a necessary step of the design [23, 28].

On the other hand, the exploitation of EM simulation tools, either throughout the entire design process or in the design closure – although necessarily – requires vast computational resources. The main issue here lies in the numerical cost associated with the high-fidelity EM analysis of the entire compact component, rather than its constitutive elements taken separately. In case of conventional EM-driven design approaches, based either on laborious parameter sweeps [27] or direct optimisation [23, 28], this becomes impractical or even prohibitive when handling computational demands of miniaturised passives.

Design difficulties related to the high computational cost of accurate EM simulation can be alleviated to some extent by using surrogate-based optimisation (SBO) techniques [29–32]. The most popular SBO approach in microwave engineering is undoubtedly space mapping (SM) [33, 34]. Unfortunately, straightforward utilisation of an algorithm such as SM is problematic in the case of miniaturised structures for several reasons. Conventional SBO methods exploit the low-fidelity model (e.g. equivalent circuit) of the entire structure [33], which is of limited accuracy because it does not account for EM couplings between tightly allocated building blocks of the structure. On the other hand, a large number of parameters make the extraction of the surrogate model parameters (as well as subsequent surrogate model optimisation) numerically complex with issues such as non-uniqueness of the extraction process and poor generalisation capability of the surrogate [31]. Also, EM simulation of the entire structure has to be performed from the very first iteration of the algorithm, which greatly affects the overall cost of the design process.

The initial attempts to partially address the aforementioned problems were described in [35, 36], where SBO techniques were exploited to solve a series of decomposed sub-problems. The numerical efficiency of the referenced methods stems from the fundamental principles of SBO technology, that is, shifting the computational burden from the expensive EM model towards a cheap and reasonably accurate replacement model (a surrogate) [37]. The major sources of computational expense are design validation and surrogate model improvement, both requiring evaluation of the EM model. The approaches of [35, 36] are suitable for a wide class of miniaturised components, however, both require inconvenient manual setup of multiple optimisation tasks, which can be unacceptable when design automation is desired.

In this paper, we introduce a novel design methodology for numerically demanding branch-line couplers (BLCs) with

miniaturised layouts composed of geometrically complex composite cells. The proposed technique enables an expedited optimisation of the entire microwave component and provides high accuracy of the results. A compact footprint of the component as well as its specified performance is achieved by adjusting designable parameters of the cells. Our approach is a two-step process. In the first stage, the composite cells are subjected to concurrent EM optimisation, without taking their mutual EM couplings into account. This is done at a low computational cost (a few evaluations of the entire BLC), due to the fact that the composite cells are electromagnetically isolated. In the second stage, BLC fine-tuning is performed, based on space-mapping-corrected surrogate model, which is constructed from cascaded local response surface approximation (RSA) models of the cells. This accounts for any cross-coupling phenomena that affect the performance of the entire component. The design procedure is initiated by a manual setup of coupler building blocks. All the following steps are fully automated. The efficiency of the proposed technique has been numerically and experimentally validated using two BLC case studies. The proposed methodology is tailored for BLC simulation-driven design, however, it can be adopted for a wider range of applications.

The paper is organised as follows. Section 2 provides a general description of the design approach, as well as a detailed mathematical formulation of its subsequent steps, that is, concurrent cell optimisation, RSA model construction and surrogate-assisted design refinement. Section 3 demonstrates the operation of the proposed method. A comprehensive comparison with benchmark optimisation methods (specifically, various space mapping algorithms), is also included. Section 4 concludes the paper.

2 Methodology

2.1 General design scheme

A step-by-step flow for the design of highly-miniaturised BLCs is shown in Fig. 1a. The computational efficiency of the proposed method is a result of concurrent optimisation of the detached composite cells (i.e. the fundamental building blocks of a compact BLC), and subsequent surrogate-assisted fine-tuning of the entire BLC. The former stage aims at reaching the optimised vectors of designable parameters pertaining to the cells of the coupler. One should note that the composite structures are geometrically dependent (to ensure a compact BLC design), but electromagnetically isolated (to lower their evaluation cost). This is extremely beneficial from the numerical perspective: neglecting of cross-coupling effects allows us to embed – in a single optimisation process – two high-fidelity, yet cheap EM models representing separate cells instead of one expensive model corresponding to the

composition of the cells of interest. Such a formulation of the optimisation task is advantageous as it leads to a solution that lies in the close vicinity of the entire BLC optimised design.

The subsequent tuning-like BLC design refinement is carried out as a surrogate-based optimisation process with a fast low-fidelity model constructed by cascading the local RSAs of the cells. In general, this is an iterative process, however, as demonstrated by the case studies (cf. Section 3), one iteration is normally sufficient.

The main advantage of our method lies in the ability to reach the optimised design within a single and fully automated process at a low computational cost. The high-fidelity EM model of the entire compact BLC is evaluated only at the tuning stage (in practice, twice: at the initial design produced by the first stage, and for the verification of the final design).

2.2 Concurrent cell optimisation

The proposed methodology offers a fully automated design of small-size BLCs. It requires, however, a manual model setup for coupler building blocks. Design considerations facilitating this process together with a wide collection of example elements for compact BLCs can be found in [26]. A conventional BLC is composed of quarter-wavelength uniform TLs of Z_0 and $Z_0/\sqrt{2}$ characteristic impedances to achieve an equal power split between the output ports (Z_0 being the system impedance) [24]. Thus, to develop a compact BLC, two complementary cells are required. They are intended to fill the interior of the BLC in a highly efficient manner with a predefined distance d between them. Geometry parameters of the cells are encoded in a parameter vector $\boldsymbol{x}$. Some of these parameters are independent; others are dependent to ensure the geometrical fit of the cells.

Formally, we can describe this dependence as $\boldsymbol{x}_1 = f_1(\boldsymbol{x})$ and $\boldsymbol{x}_2 = f_2(\boldsymbol{x})$. In practice, f_1 is a projection (i.e. $\boldsymbol{x}_1$ consists of selected components of the vector $\boldsymbol{x}$), whereas f_2 describes geometry constraints introduced to make the second cell fit into a compact coupler layout. Specific realisations of such functions are provided in Section 3.

For the purpose of cell optimisation, we use two separate high-fidelity EM models to take into account all internal EM effects existing within a composite cell, but without any cross-coupling phenomena between them. This formulation of the design problem allows us to perform a low-cost concurrent optimisation of both cells. The aggregated objective function $U(\boldsymbol{x})$ for the cells is evaluated using given design specifications and cell response vectors $R_i(\boldsymbol{x}_i)$, $i = 1, 2$ (cf. Fig. 1b).

The cells are optimised to obtain a required phase shift ϕ_c, $\arg(S_{21})$ at the operating frequency f_0 as well as to minimise the return loss $|S_{11}|$ at f_0 and around it. The task is formulated as

$$\boldsymbol{x}_c^* = \arg\min_{\boldsymbol{x}} U(\boldsymbol{x}) \tag{1}$$

where

$$U(\boldsymbol{x}) = \max_{f_0 - df \le f \le f_0 + df} \{|S_{11.1}(\boldsymbol{x}_1; f)|, |S_{11.2}(\boldsymbol{x}_2; f)|\}$$
$$+ \beta \sum_{i=1}^{2} \left[\arg\left(S_{21.i}(\boldsymbol{x}_i; f_0)\right) - \phi_c\right]^2 \tag{2}$$

here $\boldsymbol{x}$ is a composite vector of geometry parameters, $\boldsymbol{x}_i$, $i = 1, 2$, are geometry parameter vectors of the cells, β is a penalty factor (here we use $\beta = 10^4$), whereas $S_{11\ i}(\boldsymbol{x}_i; f)$ and $S_{21\ i}(\boldsymbol{x}_i; f)$ denote explicit dependence of S-parameters on frequency for the ith cell. Thus, the process (1) aims at minimising $|S_{11}|$ in the vicinity of f_0 (in practice, three frequency points are utilised: $f_0 - df$, f_0 and $f_0 + df$), while forcing $\arg(S_{21})$ to ϕ_c. The problem (1) is solved using a pattern search algorithm (cf. [37]).

2.3 RSA models

The local RSA models of the cells, utilised in the tuning process (cf. Section 2.4), are constructed in the vicinity of their optimised designs, $\boldsymbol{x}_{c.i}^*$, $i = 1, 2$, defined as $\left[\boldsymbol{x}_{c.i}^* - d\boldsymbol{x}_i, \boldsymbol{x}_{c.i}^* + d\boldsymbol{x}_i\right]$. Each
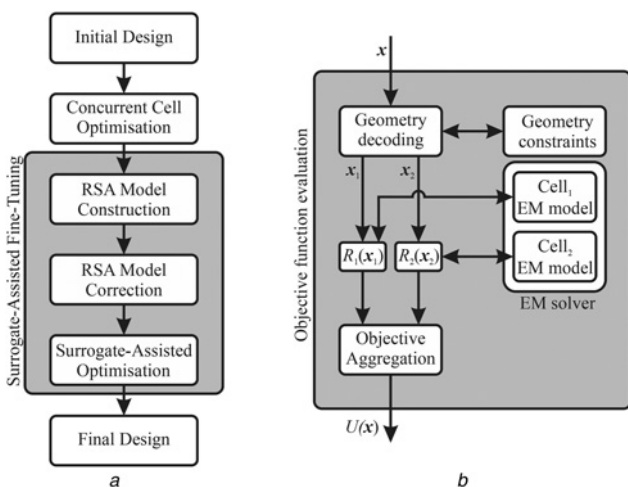

Fig. 1 *Step-by-step flow for the design of highly-miniaturised BLCs*
a Proposed design procedure of highly miniaturised BLCs
b Objective function evaluation for concurrent cell optimisation

model uses $2n_i + 1$ ($n_i = \dim(x_i)$) EM simulations of both cells at $x_{c.i}^{(0)} = x_{c.i}^*$ and at the perturbed designs

$$x_{c.i}^{(k)} = [x_{c.i.1}^*, \ldots, x_{c.i.\lceil k/2 \rceil}^* + (-1)^k \mathrm{d}x_{i.\lceil k/2 \rceil}, \ldots, x_{c.i.n_i}^*]^T,$$

$$k = 1, \ldots, 2n_i$$

where $x_{c.i.k}^*$ and $\mathrm{d}x_{i.k}$ are the kth components of the vectors $x_{c.i}^*$ and $\mathrm{d}x_i$, respectively. The RSA model $R_{c.i}(x)$ of the ith cell is a simple second-order polynomial without mixed terms

$$R_{c.i}(x) = c_{0.i} + \sum_{k=1}^{n_1} c_{k.i} x_{i.k} + \sum_{k=1}^{n_1} c_{(n+k).i} x_{i.k}^2 \qquad (3)$$

with the parameters identified as least-square solution to the linear regression problem

$$R_{c.i}(x_{c.i}^{(k)}) = R_{f.i}(x_{c.i}^{(k)}), \quad k = 0, 1, \ldots, 2n_i$$

where $R_{f.i}$ denotes the EM model of the ith cell. The RSA model R_c of the entire coupler is subsequently constructed by cascading $R_{c.i}$ using *abcd* matrix representation.

2.4 Surrogate-assisted design refinement

In order to account for EM couplings between the cells, as well as other phenomena, for example, T-junction phase shifts, final tuning of the coupler is required. The tuning procedure is realised as a surrogate-based optimisation process

$$x^{(i+1)} = \arg\min_{x} H(R_s^{(i)}(x)) \qquad (4)$$

The vectors $x^{(i)}, i = 0, 1, \ldots$ approximate the solution to the coupler design problem $x^* = \operatorname{argmin}\{x: H(R_f(x))\}$ (H encodes design specifications for the coupler), whereas $R_s^{(i)}$ is the surrogate model at iteration i. $R_s^{(i)}$ is constructed from the RSA model R_c using input space mapping [38]

$$R_s^{(i)}(x) = R_c(x + q^{(i)}) \qquad (5)$$

where $q^{(i)}$ is the input SM shift vector obtained using the usual parameter extraction procedure $q^{(i)} = \operatorname{argmin}\{q: \|R_f(x^{(i)}) - R_c(x^{(i)} + q)\|\}$, aiming at reduction of misalignment between the R_c and the EM coupler model R_f. Note that the high-fidelity model R_f is not evaluated until the tuning stage. In practice, a single iteration (4) is sufficient. The overall cost of the coupler design process is therefore very low and usually corresponds to a few simulations of the entire coupler structure including cell optimisation and construction of the RSA models.

3 Case studies

Here, we verify the methodology of Section 2. First, we formulate design specifications. The task is to design a miniaturised 3-dB BLC for operating frequency $f_0 = 1$ GHz using Taconic RF-35 ($\varepsilon_r = 3.5$, $h = 0.508$ mm and $\tan\delta = 0.0018$) as a dielectric substrate. The intended bandwidth is 0.96–1.04 GHz with return loss and isolation $|S_{11}|$, $|S_{41}| \leq -20$ dB. For comparison purposes, a conventional BLC has been designed on the basis of [26]. Its exterior dimensions are 45.6 mm × 48.1 mm.

Design requirements, imposed on each constitutive cell, are theory-based [24]. Therefore, in the first stage of the proposed design procedure, we aim at finding appropriate cell designs that approximate electrical parameters of theoretical BLC building blocks. More specifically, $|S_{11}| \leq -20$ dB at 0.96, 1 and 1.04 GHz, when loaded with 35.35 and 50 Ω resistances, respectively, and the phase shift $\phi_c = -90°$ at f_0. We use Sonnet *em* [39] to conduct all high-fidelity EM simulations. In the following design examples, the grid size is set to 0.025 mm × 0.025 mm, to provide sufficient accuracy of cell design solutions. EM simulations are performed on PC with 8-core Intel Xeon 2.5 GHz processor and 6 GB RAM. Simulation time of the entire BLC is about 90 min for design case 1, and 110 min for design case 2 (both with adaptive frequency

sweep). Single frequency simulation of a single cell is, on average, about 15 and 18 s for design case 1 and design case 2, respectively.

3.1 Design case I

For the first example, we use cell parameterisation shown in Fig. 2. It can be observed that the complementary cells are arranged according to their intended placement in the target BLC. Dimensions of horizontal and vertical cells (denoted Cell_1 and Cell_2, respectively) are given by vectors x_1 and x_2. All parameters of Cell_1, x_1, x_2, …, x_7, are independent, whereas Cell_2 is described by both independent, x_8, x_9, …, x_{12} and dependent, y_1, y_2 and y_3, parameters. The latter depend on specific parameters of Cell_1 and the predefined distance d between the cells. Referring to the notation from Section 2.2, parameterisation of Cell_1 and Cell_2 is given by: $f_1(x) = f_1([x_1 \ x_2 \ \ldots \ x_{12}]^T) = [x_1 \ x_2 \ \ldots \ x_7]^T$ and $f_2(x) = f_2([x_1 \ x_2 \ \ldots \ x_{12}]^T) = [x_8 \ x_9 \ \ldots \ x_{12} \ y_1 \ y_2 \ y_3]^T$, where $y_1 = 0.5 \cdot (x_7 + d/2 - x_8 - 2 \cdot x_{10} - 2.5 \cdot x_{12})$, $y_2 = x_1 + x_3 + x_4 + x_6 - d - x_{12}$ and $y_3 = x_8 + x_{12} - d$. This has been done to preserve consistency of the dimensions and high compression of the BLC. In this example, $d = 0.2$ mm.

The cells of Fig. 2 have been subjected to concurrent optimisation, starting from

$$x_c^{(0)} = [0.1 \ 1.9 \ 4 \ 0.1 \ 5.7 \ 0.1 \ 4 \ 0.1 \ 1.15 \ 0.1 \ 5.05 \ 0.1]^T$$

and yielding

$$x_c^* = [0.45 \ 1.9 \ 3.325 \ 0.225 \ 1.55 \ 0.125 \ 8.05 \ 0.1 \ 1.15 \ 0.1 \ 0.4 \ 1]^T$$

Corresponding constrained optima for individual cells are

$$f_1(x_c^*) = [0.45 \ \ 1.9 \ \ 3.325 \ \ 0.225 \ \ 1.55 \ \ 0.125 \ \ 8.05]^T \text{ mm}$$

and

$$f_2(x_c^*) = [0.1 \ \ 1.15 \ \ 0.1 \ \ 0.4 \ \ 1 \ \ 2.675 \ \ 2.925 \ \ 0.9]^T \text{ mm}$$

The EM evaluation of the entire BLC at the design produced in this step demonstrates a degraded performance because of cross-coupling effects that occur between adjacent cells. This is addressed by the subsequent fine-tuning procedure. For that purpose, we construct local RSA models of the respective optimised cells and use them to develop the coarse model of the entire BLC (by cascading *ABCD* matrices of the corresponding building blocks). Next, the execution of the surrogate-assisted design refinement algorithm follows.

The differences between pre- and post-tuning BLC designs are illustrated in Figs. 3a and b. One can see that the final post-tuning BLC design solution, given

$$f_1(x^*) = [0.475 \ \ 1.9 \ \ 3.25 \ \ 0.225 \ \ 1.5 \ \ 0.125 \ \ 8.05]^T \text{ mm}$$

and

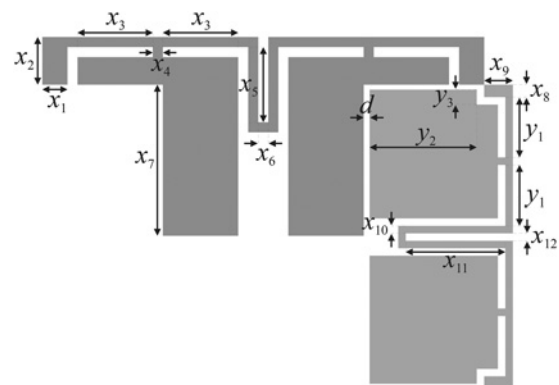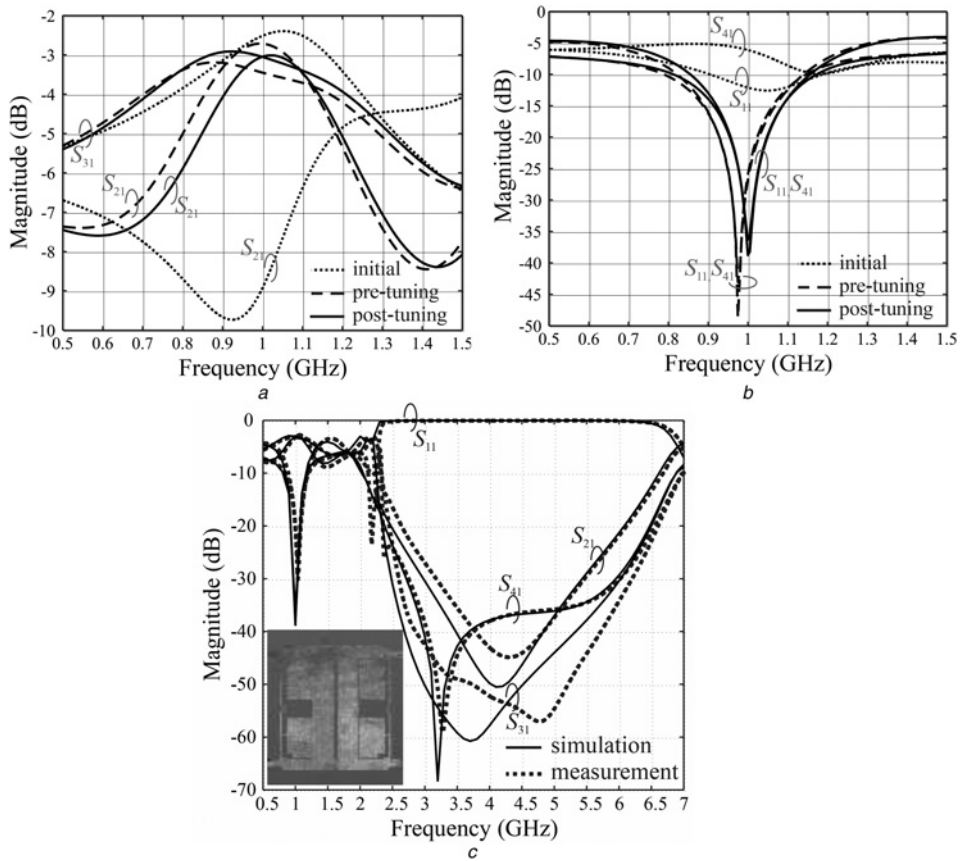$$f_2(x^*) = [0.125 \ 1.15 \ 0.125 \ 0.375 \ 0.95 \ 2.7 \ 2.925 \ 0.875]^T \text{ mm}$$

Fig. 2 *Design case I: parameterised layouts of $Cell_1$ (dark grey colour, port impedance $Z_0 = 35.35\ \Omega$) and $Cell_2$ (light grey colour, port impedance $Z_0 = 50\ \Omega$)*

Fig. 3 *Design case I*

a and *b* Initial (dotted line), pre-tuning (dashed line), and post-tuning (solid line) BLC *S*-parameters
c Post-tuning BLC broadband performance – simulation (solid line) against measurement (dotted line)

shows a perfect performance in contradiction to the pre-tuning BLC design. The final design has been manufactured and measured.

The measurement results shown in Fig. 3*c* are comparable to the simulated performance, where minor discrepancy is most likely because of the lack of metal surface roughness and dielectric anisotropy included in EM simulation [40], as well as geometrical differences (fabrication tolerance) between the model and prototype.

It should be emphasised that the final BLC has reached 83.7% scale of size reduction as well as ideal characteristics confirmed by measurement data – all at a low computational cost corresponding to about 5.6 full-wave analyses of the final compact BLC model. The design cost breakdown is the following: concurrent cell

optimisation (150 cell evaluations at three frequencies each, ∼225 min in total), data acquisition for RSA model construction (21 cell evaluations at ten frequencies each, ∼105 min in total), and two simulations of the entire coupler (∼180 min). The overall design cost of the proposed method is ∼510 min. One should bear in mind that a direct optimisation would require several hundred such evaluations, which is virtually infeasible.

For the sake of comparison, the coupler was also optimised using benchmark techniques, here, conventional space mapping algorithms [38]. The equivalent circuit shown in Fig. 4*a* was used as an underlying coarse model implemented in Agilent ADS [41]. The initial design was obtained by optimising the coarse model $R_{circuit}$.
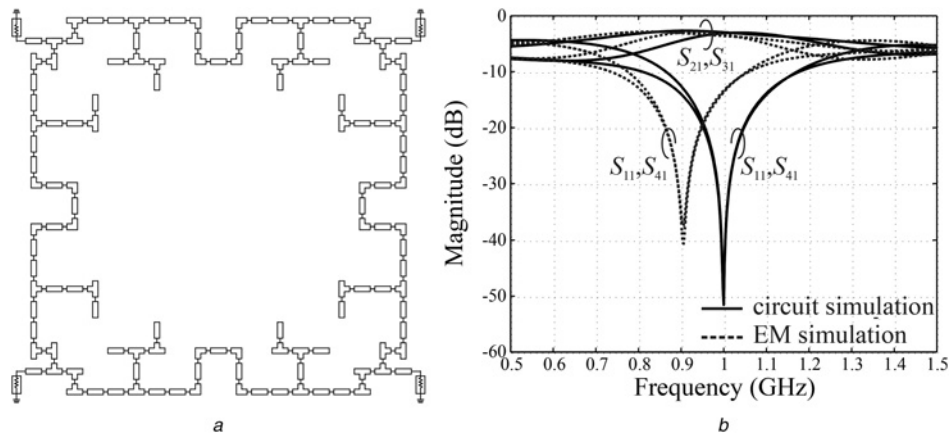
Fig. 4 *Design case I*

a Equivalent circuit ADS implementation ($R_{circuit}$) of the compact BLC
b Performance comparison of the compact BLC optimised coarse model ($R_{circuit}$) and its corresponding EM model

Table 1 BLC optimisation (design case I): comparison with benchmark methods

Algorithm	Final design at 1 GHz			Design cost	
	$|S_{21}-S_{31}|$, dB	Return loss $|S_{11}|$, dB	Isolation $|S_{41}|$, dB	Number of coupler simulations	Total cost[a]
this work	0.01	−39	−36	2	∼6
SM (i)[b]	0.5	−24	−25.5	6	∼8
SM (ii)[c]	0.01	−26	−26.5	6	∼8
SM (iii)[d]	0.2	−51	−51	7	∼9
SM (iv)[e]	0.6	−25	−24	6	∼9

[a]Total design cost expressed as the number of equivalent coupler simulations; includes all operations (cell optimisation, surrogate optimisation and extraction of SM model parameters).
[b]Input SM; the surrogate $R_{circuit}(x+c)$ ($R_{circuit}$ is the equivalent circuit model).
[c]Implicit SM with nine dielectric permittivities as preassigned parameters.
[d]Implicit SM with nine substrate heights as preassigned parameters.
[e]Implicit SM with 18 parameters (substrate heights and permittivities).

This itself is a straightforward adaptation of the theory-based design approach of [2–23]. To illustrate its minor usefulness in the design of highly miniaturised microwave components and the need for subsequent EM fine-tuning, we compare in Fig. 4b the performance of the optimised coarse model and its corresponding EM model. One can notice a considerable shift in the operating frequency of the optimised BLC because of the insufficient accuracy of the model.

For the purpose of comprehensive assessment of our method, we compared it against four different versions of the SM algorithm: (i) input SM with the surrogate model defined as $R_s(x) = R_{circuit}(x+c)$ (the shift vector c obtained through usual parameter extraction process [33]); (ii) implicit SM [38] with nine preassigned parameters (substrate heights); (iii) implicit SM with nine substrate dielectric permittivities as preassigned parameters; and (iv) implicit SM with 18 preassigned parameters (both substrate heights and permittivities). The SM surrogate model parameters were extracted using the most recent design only. This was necessary to reduce the computational cost of the parameter extraction process. The results for the proposed and all benchmark methods have been gathered in Table 1.

It can be observed that the computational cost of the design process is the lowest for the methodology presented in this paper compared to all considered versions of space mapping. In terms of performance, our approach ensures the most consistent results in terms of all performance parameters (only 0.01 dB difference between coupling and transmission at the frequency of operation, and almost −40 dB of both return loss and isolation). SM algorithms produce results that are generally worse in terms of return loss and isolation (except SM (iii)) as well as the difference between coupling and transmission (except SM (ii), where the results are comparable). The biggest problem with SM is the right choice of the surrogate model setup: the results of all versions (i)–(iv) are inconsistent with each other. Of course, the optimum SM setup is unknown beforehand. This is a major drawback, because the overall success of the method depends on the experience of the user, which is not something that can be assumed generally available.

3.2 Design case II

In the second example, we use cell parameterisation of Fig. 5, where $d = 0.4$ mm, and the geometrical description is given by: $f_1(x) = f_1([x_1 \ x_2 \ ... \ x_{12}]^T) = [x_1 \ x_2 \ ... \ x_7]^T$ and $f_2(x) = f_2([x_1 \ x_2 \ ... \ x_{12}]^T) = [x_8 \ x_9 \ ... \ x_{12} \ y_1 \ y_2]^T$, where $y_1 = x_1 + x_3 + 2 \cdot x_4 + 3 \cdot x_5 + x_9 + x_{12} - d$ and $y_2 = -x_2 + x_4 + x_5 + x_6 - x_8 - x_{10} - 3.5 \cdot x_{11} - 3 \cdot x_{12} + d/2$. The initial design is given by

$$x_c^{(0)} = [0.1 \ \ 1.9 \ \ 2 \ \ 0.1 \ \ 0.1 \ \ 6 \ \ 2 \ \ 0.1 \ \ 1.15 \ \ 2 \ \ 0.1 \ \ 0.1]^T$$
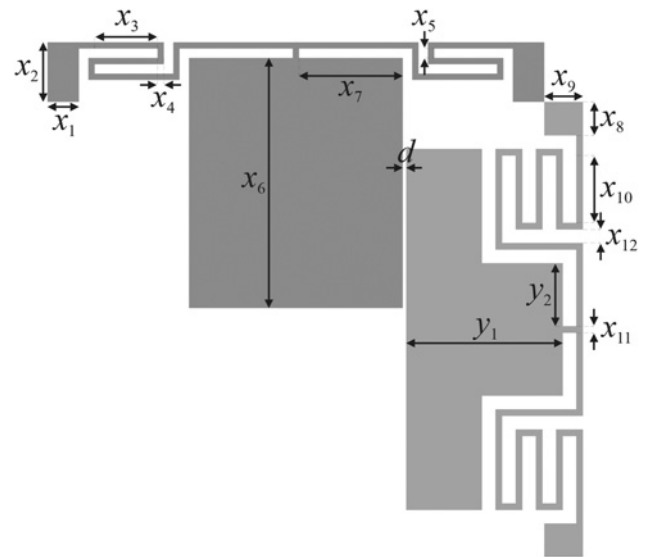
Fig. 5 *Design case II: parameterised layouts of Cell₁ (dark grey colour, port impedance $Z_0 = 35.35 \ \Omega$) and Cell₂ (light grey colour, port impedance $Z_0 = 50 \ \Omega$)*

The first stage of our method results in

$$x_c^* = [0.6 \ \ 1.9 \ \ 2 \ \ 0.2 \ \ 0.175 \ \ 7.975 \ \ 3.3 \ \ 0.5 \ \ 1.15 \ \ 1.1 \ \ 0.2 \ \ 0.4]^T$$

with the corresponding constrained optima

$$f_1(x_c^*) = [0.6 \ \ 1.9 \ \ 2 \ \ 0.2 \ \ 0.175 \ \ 7.975 \ \ 3.3]^T \text{mm}$$

and

$$f_2(x_c^*) = [0.5 \ \ 1.15 \ \ 1.1 \ \ 0.2 \ \ 0.4 \ \ 3.875 \ \ 3.15]^T \text{mm}$$

The tuning phase yields

$$f_1(x^*) = [0.6 \ \ 1.9 \ \ 1.975 \ \ 0.2 \ \ 0.15 \ \ 7.925 \ \ 3.25]^T \text{mm}$$

and

$$f_2(x^*) = [0.5 \ \ 1.15 \ \ 1.125 \ \ 0.2 \ \ 0.325 \ \ 3.85 \ \ 3.275]^T \text{mm}$$

The comparison between pre- and post-tuning BLC designs are given in Figs. 6a and b. One can see that the SBO correction technique applied at this stage greatly improves the performance of the coupler to the point where no other EM fine-tuning is necessary. This is also confirmed by the measurement results given is Fig. 6c. Transmission characteristics of the manufactured BLC are in agreement with simulation data, although some minor differences can be observed, most likely because of the simplified simulation: no SMA connectors were included, isotropic dielectric substrate as well as smooth metallisation were used, no fabrication tolerance was considered. It should be reiterated that the proposed method enabled a low-cost design of a highly miniaturised BLC (87.4% of size reduction), which demonstrates almost ideal characteristics. The overall design cost of the technique introduced in this work is ∼616 min (this translates into about 5.6 evaluations of the entire BLC) and consists of the following: concurrent cell optimisation (150 cell evaluations at three frequencies each, ∼270 min in total), data acquisition for RSA model construction (21 cell evaluations at ten frequencies each, ∼126 min in total), and two simulations of the entire coupler (∼220 min).
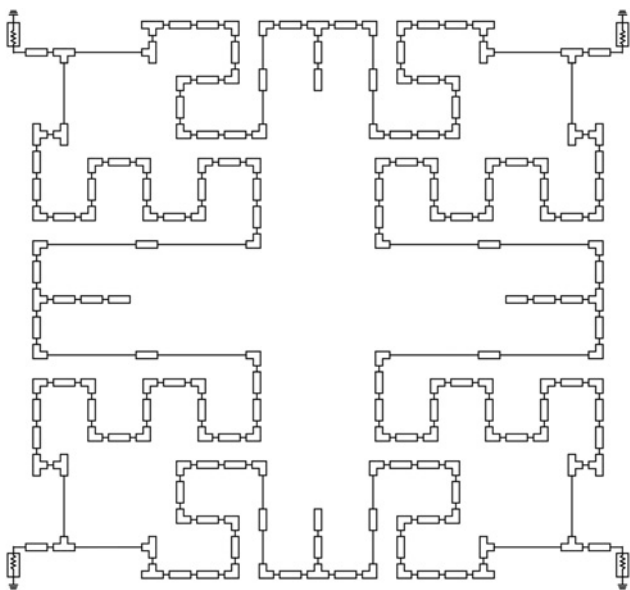
Similarly as for the previous example, the proposed design approach was compared to conventional space mapping algorithms. The equivalent circuit $R_{circuit}$ of the coupler used by SM is shown in Fig. 7. As before, the initial design was obtained by optimising $R_{circuit}$. Again, we examine four different versions of
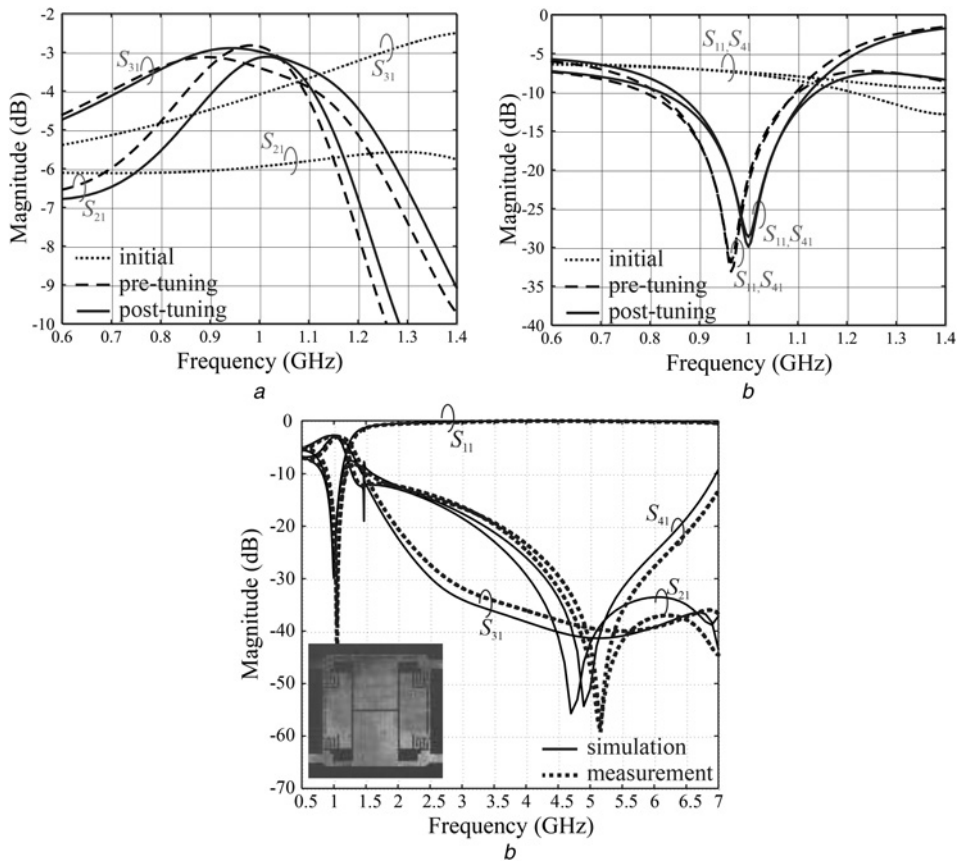
Fig. 6 *Design case II*

a and *b* Initial (dotted line), pre-tuning (dashed line) and post-tuning (solid line) BLC S-parameters
c Post-tuning BLC broadband performance – simulation (solid line) against measurement (dotted line)

the SM algorithm: (i) input SM; (ii) implicit SM with substrate heights as preassigned parameters; (iii) implicit SM with dielectric permittivities as preassigned parameters; and (iv) implicit SM with both substrate heights and permittivities as preassigned parameters. The results for the proposed and all benchmark methods can be found in Table 2.

Fig. 7 *Equivalent circuit ADS implementation ($R_{circuit}$) of the compact BLC from design case II*

The results are consistent with what was obtained for the first example. Specifically, the computational cost of the design process is the lowest for the methodology presented here. Performance-wise, our approach ensures the most consistent results (0.05 dB difference between coupling and transmission at the frequency of operation, and about −30 dB of both return loss and isolation). SM algorithms produce results that are generally worse either in terms of return loss and isolation or the difference between coupling and transmission. As before, the most serious issue is dependence of SM performance on the particular choice of the SM surrogate model.

Table 2 BLC optimisation (design case II): comparison with benchmark methods

Algorithm	Final design at 1 GHz			Design cost	
	$|S_{21}-S_{31}|$, dB	Return loss $|S_{11}|$, dB	Isolation $|S_{41}|$, dB	Number of coupler simulations	Total cost[a]
this work	0.05	−30	−28.5	2	~6
SM (i)[b]	0.35	−37	−25	7	~9
SM (ii)[c]	0.05	−28	−25.5	6	~8
SM (iii)[d]	0.15	−28	−27	6	~8
SM (iv)[e]	0.45	−23	−25	9	~13

[a]Total design cost expressed as the number of equivalent coupler simulations; includes all operations (cell optimisation, surrogate optimisation and extraction of SM model parameters).
[b]Input SM; the surrogate $R_{circuit}(\boldsymbol{x} + \boldsymbol{c})$ ($R_{circuit}$ is the equivalent circuit model).
[c]Implicit SM with nine dielectric permittivities as preassigned parameters.
[d]Implicit SM with nine substrate heights as preassigned parameters.
[e]Implicit SM with 18 parameters (substrate heights and permittivities).

4 Conclusions

A simple, automated and reliable procedure for fast design optimisation of compact branch-line couplers has been presented. Our methodology addresses the two fundamental problems of conventional techniques for miniaturised microwave component design: (i) inaccuracy because of the relying on equivalent circuit models (and thus neglecting cross-coupling effects), (ii) high computational cost of EM-based design closure [necessary in any case because of (i)]. The proposed technique is rigorously formulated and therefore straightforward to implement and automate. The final design is obtained in a single tuning iteration so that convergence problems, typical for other techniques (including surrogate-based approaches) are not an issue. Comparison with several versions of space mapping indicates consistent performance and no ambiguity due to selection of a specific coarse model correction type. Finally, the final designs of compact BLCs are obtained at a low computational cost (several hours of CPU time).

The proposed method is also suitable for handling similar design problems, where the target circuit can be decomposed into strictly specified elements. This includes multi-section matching transformers, Wilkinson power dividers, Lange or rat-race couplers, to name just a few. The most important advantage of our approach, besides its low computational cost, is that it allows convenient handling of EM cross-coupling effects between the structure cells (which cannot be properly accounted for using simplified means, e.g. equivalent circuit models). At the same time, potential limitation of the method is when the couplings between the adjacent building blocks are extremely strong. In such cases, discrepancies between the aggregated approximation model and the entire (EM-simulated) structure might not be accommodated through space mapping.

5 Acknowledgment

6 References

1 Gilmore, R., Besser, L.: 'Practical RF circuit design for modern wireless systems' (Artech House, Norwood, MA, 2003)
2 Xu, H.-X., Wang, G.-M., Lu, K.: 'Microstrip rat-race couplers', *IEEE Microw. Mag.*, 2011, **12**, (4), pp. 117–129
3 Ahn, H.-R., Bumman, K.: 'Toward integrated circuit size reduction', *IEEE Microw. Mag.*, 2008, **9**, (1), pp. 65–75
4 Liao, S.-S., Sun, P.-T., Chin, N.-C., Peng, J.-T.: 'A novel compact-size branch-line coupler', *IEEE Microw. Wirel. Compon. Lett.*, 2005, **15**, (9), pp. 588–590
5 Liao, S.-S., Peng, J.-T.: 'Compact planar microstrip branch-line couplers using the quasi-lumped elements approach with nonsymmetrical and symmetrical T-shaped structure', *IEEE Trans. Microw. Theory Tech.*, 2006, **54**, (9), pp. 3508–3514
6 Tang, C.-W., Chen, M.-G.: 'Synthesizing microstrip branch-line couplers with predetermined compact size and bandwidth', *IEEE Trans. Microw. Theory Tech.*, 2007, **55**, (9), pp. 1926–1934
7 Jung, S.-C., Negra, R., Ghannouchi, F.M.: 'A design methodology for miniaturized 3-dB branch-line hybrid couplers using distributed capacitors printed in the inner area', *IEEE Trans. Microw. Theory Tech.*, 2008, **56**, (12), pp. 2950–2953
8 Ahn, H.-R.: 'Modified asymmetric impedance transformers (MCCTs and MCVTs) and their application to impedance-transforming Three-Port 3-dB power dividers', *IEEE Trans. Microw. Theory Tech.*, 2011, **59**, (12), pp. 3312–3321
9 Tseng, C.-H., Chang, C.-L.: 'A rigorous design methodology for compact planar branch-line and rat-race couplers with asymmetrical T-structures', *IEEE Trans. Microw. Theory Tech.*, 2012, **60**, (7), pp. 2085–2092
10 Ahn, H.-R., Nam, S.: 'Compact microstrip 3-dB coupled-line ring and branch-line hybrids with new symmetric equivalent circuits', *IEEE Trans. Microw. Theory Tech.*, 2013, **61**, (3), pp. 1067–1078
11 Bekasiewicz, A., Kurgan, P.: 'A compact microstrip rat-race coupler constituted by nonuniform transmission lines', *Microw. Opt. Tech. Lett.*, 2014, **56**, (4), pp. 970–974

12 Eccleston, K.W., Ong, S.H.M.: 'Compact planar microstripline branch-line and rat-race couplers', *IEEE Trans. Microw. Theory Tech.*, 2003, **51**, (10), pp. 2119–2125
13 Chuang, M.-L.: 'Miniaturized ring coupler of arbitrary reduced size', *IEEE Microw. Wirel. Compon. Lett.*, 2005, **15**, (1), pp. 16–18
14 Chun, Y.-H., Hong, J.-S.: 'Compact wide-band branch-line hybrids', *IEEE Trans. Microw. Theory Tech.*, 2006, **54**, (2), pp. 704–709
15 Kuo, J.-T., Wu, J.-S., Chiou, Y.-C.: 'Miniaturized rat race coupler with suppression of spurious passband', *IEEE Microw. Wirel. Compon. Lett.*, 2007, **17**, (1), pp. 46–48
16 Mondal, P., Chakrabarty, A.: 'Design of miniaturised branch-line and rat-race hybrid couplers with harmonics suppression', *IET Microw. Antennas Propag.*, 2009, **3**, (1), pp. 109–116
17 Ahn, H.-R., Kim, B.: 'Small wideband coupled-line ring hybrids with no restriction on coupling power', *IEEE Trans. Microw. Theory Tech.*, 2009, **57**, (7), pp. 1806–1817
18 Sun, K.-O., Ho, S.-J., Yen, C.-C., van der Weide, D.: 'A compact branch-line coupler using discontinuous microstrip lines', *IEEE Microw. Wirel. Compon. Lett.*, 2005, **15**, (8), pp. 501–503
19 Lee, H.-S., Choi, K., Hwang, H.-Y.: 'A harmonic and size reduced ring hybrid using coupled lines', *IEEE Microw. Wirel. Compon. Lett.*, 2005, **17**, (4), pp. 259–261
20 Tseng, C.-H., Chen, H.-J.: 'Compact rat-race coupler using shunt-stub-based artificial transmission lines', *IEEE Microw. Wirel. Compon. Lett.*, 2008, **18**, (11), pp. 734–736
21 Wang, C.-W., Ma, T.-G., Yang, C.-F.: 'A new planar artificial transmission line and its applications to a miniaturized butler matrix', *IEEE Trans. Microw. Theory Tech.*, 2007, **55**, (12), pp. 2792–2801
22 Ahn, H.-R., Nam, S.: 'Wideband microstrip coupled-line ring hybrids for high power-division ratios', *IEEE Trans. Microw. Theory Tech.*, 2013, **61**, (5), pp. 1768–1780
23 Tsai, K.-Y., Yang, H.-S., Chen, J.-H., Chen, Y.-J.: 'A miniaturized 3 dB branch-line hybrid coupler with harmonics suppression', *IEEE Microw. Wirel. Compon. Lett.*, 2011, **21**, (10), pp. 537–539
24 Collin, R.E.: 'Foundations for microwave engineering' (John Wiley & Sons Inc., New York, 2001)
25 Gu, J., Sun, X.: 'Miniaturization and harmonic suppression rat-race coupler using C-SCMRC resonators with distributive equivalent circuit', *IEEE Microw. Wirel. Compon. Lett.*, 2005, **15**, (12), pp. 880–882
26 Kurgan, P., Filipcewicz, J., Kitlinski, M.: 'Development of a compact microstrip resonant cell aimed at efficient microwave component size reduction', *IET Microw. Antennas Propag.*, 2012, **6**, (12), pp. 1291–1298
27 Kurgan, P., Kitlinski, M.: 'Novel doubly perforated broadband microstrip branch-line couplers', *Mirow. Opt. Tech. Lett.*, 2009, **51**, (9), pp. 2149–2152
28 Kurgan, P., Kitlinski, M.: 'Doubly miniaturized rat-race hybrid coupler', *Mirow. Opt. Tech. Lett.*, 2011, **53**, (6), pp. 1242–1244
29 Queipo, N.V., Haftka, R.T., Shyy, W., Goel, T., Vaidynathan, R., Tucker, P.K.: 'Surrogate based analysis and optimization', *Progr. Aerosp. Sci.*, 2005, **41**, (1), pp. 1–28
30 Yelten, M.B., Zhu, T., Koziel, S., Franzon, P.D., Steer, M.B.: 'Demystifying surrogate modeling for circuits and systems', *IEEE Circuits Syst. Mag.*, 2012, **12**, (1), pp. 45–63
31 Koziel, S., Yang, X.S. (Eds.): 'Computational optimization, methods and algorithms' (Series: Studies in Computational Intelligence) (Springer, 2011), vol. 356
32 Koziel, S.: 'Efficient optimization of microwave circuits using shape-preserving response prediction'. IEEE MTT-S Int. Microwave Symp. Dig, Boston, MA, 2009, pp. 1569–1572
33 Bandler, J.W., Cheng, Q.S., Dakroury, S.A., *et al.*: 'Space mapping: the state of the art', *IEEE Trans. Microw. Theory Tech.*, 2004, **52**, (1), pp. 337–361
34 Liu, X., Wang, G., Liu, J.: 'A wideband model of on-chip CMOS interconnects using space-mapping technique', *Int. J. RF Microw. CAE*, 2011, **21**, (4), pp. 439–445
35 Bekasiewicz, A., Kurgan, P., Kitlinski, M.: 'New approach to a fast and accurate design of microwave circuits with complex topologies', *IET Microw. Antennas Propag.*, 2012, **6**, (14), pp. 1616–1622
36 Kurgan, P., Bekasiewicz, A.: 'A robust design of a numerically demanding compact rat-race coupler', *Microw. Opt. Tech. Lett.*, 2014, **56**, (5), pp. 1259–1263
37 Koziel, S., Leifsson, L., Zhang, Q.J. (Eds.): 'Surrogate-based optimization', in Koziel, S., Yang, X.S., Zhang, Q.J. (Eds.): 'Simulation-driven design optimization and modeling for microwave engineering' (Imperial College Press, 2012), pp. 41–80
38 Koziel, S., Bandler, J.W., Madsen, K.: 'Towards a rigorous formulation of the space mapping technique for engineering design'. Proc. Int. Symp. Circuits, Systems, ISCAS, 2005, vol. 1, pp. 5605–5608
39 Sonnet, version 14.54. Sonnet Software, North Syracuse, NY, United States, 2013
40 Rautio, J.C., Rautio, B.J., Arvas, S., Horn III, A.F., Reynolds, J.W.: 'The effect of dielectric anisotropy and metal surface roughness'. Proc. Asia-Pacific Microwave Conf. (APMC), 2010, pp. 1777–1780
41 Agilent ADS, ver. 2011, Agilent Technologies, 1400 Fountaingrove Parkway, Santa Rosa, CA 95403-1799, 2011